Selective Immunoreactivities of Kidney Basement Membranes to Monoclonal Antibodies against Laminin: Localization of The End of the Long Arm and the Short Arms to Discrete Microdomains

Dale R. Abrahamson,*‡ Michael H. Irwin,* Patricia L. St. John,* Elizabeth W. Perry,* Mary Ann Accavitti,§ Louis W. Heck,§ and John R. Couchman*

*Department of Cell Biology and Anatomy, ‡Nephrology Research and Training Center, and §Department of Medicine, University of Alabama at Birmingham, UAB Station, Birmingham, Alabama 35294

Abstract. To examine the ultrastructural distribution of laminin within kidney basement membranes, we prepared rat anti-mouse laminin mAbs to use in immunolocalization experiments. Epitope domains for these mAbs were established by immunoprecipitation, immunoblotting, affinity chromatography, and rotary shadow EM. One mAb bound to the laminin A and B chains on blots and was located to a site ~15 nm from the long arm-terminal globular domain as shown by rotary shadowing. Conjugates of this long arm-specific mAb were coupled to horseradish peroxidase (HRP) and intravenously injected into mice. Kidney cortices were fixed for microscopy 3 h after injection. HRP reaction product was localized irregularly within the renal glomerular basement membrane (GBM) and throughout mesangial matrices. In addition, this mAb bound in linear patterns specifically to the laminae rarae of basement membranes of Bowman's capsule and proximal tubule. This indicates the presence of the long arm immediately beneath epithelial cells in these sites. The laminae densae of these basement membranes were negative by this protocol. In contrast, the lamina rara and densa of distal tubular basement membranes (TBM) were both heavily labeled with this mAb. A different ultrastructural binding pattern was seen with eight other mAbs, including two that mapped to different sites on the short arms by rotary shadowing and five that blotted to a large pepsin-resistant laminin fragment (P1). These latter mAbs bound weakly or not at all to GBM but all bound throughout mesangial matrices. In contrast, discrete spots of HRP reaction product were seen across all layers of Bowman's capsule BM and proximal TBM. These same mAbs, however, bound densely across the full width of distal TBM. Our findings therefore show that separate strata of different basement membranes are variably immunoreactive to these laminin mAbs. The molecular orientation or integration of laminin into the three dimensional BM meshwork therefore varies with location. Alternatively, there may be a family of distinct laminin-like molecules distributed within basement membranes.

BASEMENT membranes underlie epithelial cells and surround all muscle cells, Schwann cells of peripheral nerves, and fat cells. These widespread sheets of extracellular matrix define tissue boundaries and represent barriers to the passage of metastatic and other cells and macromolecules between tissue compartments. In addition, basement membranes orient attached cells and are important for pattern development during organogenesis and wound repair (reviewed in references 2 and 60). Ultrastructurally, basement membranes resemble a finely granular mat of narrow fibers that classically have been described as having two layers: (*a*) an electron lucent layer (lamina lucida or rara) immediately beneath the cells they are supporting and (*b*) a subjacent electron dense layer (lamina densa). Some reports on freeze-substituted tissues, however, have failed to identify a lamina lucida, thus raising questions as to whether this layer might be a fixation artifact (20). Nevertheless, basement membranes are certainly polarized in the sense that their upper surfaces contact cells and their lower surfaces face and are attached to the underlying interstitial connective tissue.

Considerable progress has been made in recent years in understanding the molecular composition of basement membranes and cDNAs for the major structural glycoproteins, collagen type IV and laminin, have now been cloned and partially sequenced (7, 8, 13, 24, 30, 44, 49, 50, 53–55, 58). When viewed in the electron microscope, laminin is shaped as an asymmetric cross with three short arms and one long arm, all terminating in globular domains (16). The molecule

synthesized by parietal endoderm cells and present in the Englebreth-Holm-Swarm tumor matrix is composed of three different polypeptide chains designated A, B1, and B2 having a combined molecular mass of ~850,000 D (26, 53–55). Most evidence now indicates that each short arm is formed by the NH_2 terminus region of one of the polypeptides and that the center of the cross is where the three chains become associated through numerous disulfide bonds (reviewed in reference 40). The long arm contains COOH-terminal regions of all three chains wound together in a coiled coil (7, 48). Fragments of laminin have been obtained after treatment with various proteases and several functional domains have been identified. Digestion with pancreatic elastase (46) yields, among some smaller products, a 140,000 M_r, piece of laminin corresponding to the end of the long arm including the terminal globule (48). This fragment, designated E8, has been shown to bind heparin and heparan sulfate proteoglycans and promote neurite outgrowth in vitro (13, 15, 17, 40). Pepsin treatment yields a large, enzyme-resistant fragment designated P1 (52, 62). This three-armed structure lacks the globular domains seen in intact laminin and corresponds to the center of the laminin cross (16, 52). In addition, the P1 fragment contains cell-binding activities for certain cells in culture (61). The ends of the arms of intact laminin are believed to bind specifically to collagen type IV and possibly to other laminin molecules (9, 10, 64). Laminin is therefore considered to be a cell attachment glycoprotein as well as a major structural element of basement membranes.

Despite recent advances, however, we do not yet understand the architecture of basement membranes at the molecular level. One approach to this problem has been to attempt to reconstruct basement membranes in vitro by admixing various preparations of purified basement membrane components. Based on electron microscopy of rotary shadowed replicas of such mixtures, several models have been proposed (35, 65). Although they differ in detail, most models describe a core, three-dimensional meshwork of polymerized collagen type IV decorated systematically with laminin and heparan sulfate proteoglycans which themselves assume specific orientations. Another approach has been to label tissues immunohistochemically with antibodies specific for the various basement membrane components. Most results now indicate that collagen IV, laminin, heparan sulfate proteoglycans, and entactin/nidogen are present throughout the full width of basement membranes (2, 3, 36, 60). These immunohistochemical results are consistent with what is known about the structure of laminin. When considering the size of the fully extended molecule (110 nm across the long axis × 70 nm across the short arms [16]), laminin in an elongated conformation is clearly large enough to span basement membranes, most of which are 50–100 nm thick. There is little information, however, on the spatial configurations of laminin or any of the other basement membrane macromolecules in vivo.

The purpose of the experiments described here was to prepare and characterize mAbs against different structural domains of laminin. We then used these mAbs in conjunction with immunoelectron microscopy to determine the ultrastructural distribution of these laminin domains within basement membranes.

Materials and Methods

Enzymatic Digestion of Laminin

Laminin was purified from the mouse Englebreth-Holm-Swarm tumor by sequential salt extraction, DEAE chromatography, and gel filtration using a modification of the method originally reported by Timpl et al. (62) as previously described (5).

At a concentration of 0.45 mg/ml in 10% acetic acid, laminin was digested with porcine stomach pepsin (3,200 U/mg; Sigma Chemical Co., St. Louis, MO) at an enzyme/substrate ratio of 1:40 (wt/wt) for 16 h at 4°C. The reaction was stopped by dialysis into PBS, pH 7.3. The pepsin digest was then chromatographed over a column of Sephacryl S-300 (Pharmacia Fine Chemicals, Piscataway, NJ) to separate the P1 fragment.

For elastase digestion, 0.45 mg/ml laminin in 0.05 M ammonium bicarbonate, pH 7.8, was treated with porcine pancreatic elastase (127 U/mg; Serva Fine Biochemicals, Westbury, NY) at an enzyme/substrate ratio of 1:500 (wt/wt) for 4 h at 37°C. The reaction was terminated by the addition of PMSF to a final concentration of 0.2 M. In some cases, the elastase digest was further processed by passage over a column of heparin-Sepharose (Pharmacia Fine Chemicals). Bound protein was eluted with the addition of 0.5 M NaCl in 0.05 M ammonium bicarbonate, pH 7.8.

Production of Rat Anti-Laminin mAbs

A Sprague-Dawley rat was immunized according to previously published procedures (39) with slight modifications. The rat received injections of 200 μg of purified laminin emulsified with an equal volume of complete Freund's adjuvant, distributing the antigen subcutaneously into the rear footpads and inguinal region. Injections of antigen in saline were repeated four times at 3-d intervals. 1 d after the last immunization, popliteal and inguinal lymph nodes were removed, prepared as a cell suspension, and fused with the nonsecreting mouse myeloma cell line P3X63AB.653 as described (33). 14 d after fusion, tissue culture supernatants were screened by ELISA on laminin-coated microtiter plates and those that were positive were screened further by indirect immunofluorescence on cryostat sections of mouse kidney. Clones that were intensely positive by both assays were subcloned by limiting dilution, expanded to high density, and injected into pristane-primed nude mice to produce ascites fluid. mAb subclass identity was established by ELISA using Ig-subclass specific antibodies (Southern Biological Associates, Birmingham, AL).

Characterization of Monoclonal Anti-Laminin IgGs

Immunoglobulins from ascites fluids were twice precipitated with the addition of equal volumes of saturated ammonium sulfate, pH 7.8, resuspended in 0.02 M phosphate, pH 7.3, and dialyzed extensively against the same buffer. IgGs were then obtained by chromatography over Whatman DE52 anion exchange cellulose (Pierce Chemical Co., Rockford, IL) and aliquoted and stored at −20°C. Affinities of the separate mAbs for laminin were evaluated in inhibition ELISAs as described before for polyclonal anti-laminin IgGs (1).

Immunoprecipitation of Laminin

Murine PYS-2 cells (37), at a density of 0.5 × 10^6/35 mm dish, were plated overnight in DME (Mediatech, Inc., Herndon, VA) containing 10% FCS (Flow Laboratories, McLean, VA). Confluent monolayers were washed 16 h later with serum-free methionine-depleted DME (1 μg/ml), either with or without 10 μg/ml tunicamycin (Boehringer Mannheim Biochemicals, Indianapolis, IN). The cells were then incubated with 150 μCi/dish of [^{35}S]methionine (1,086 Ci/mmol) (Du Pont NEN Research Products, Boston, MA) in 1.0 ml DME containing 1 μg/ml unlabeled methionine, with or without 10 μg/ml tunicamycin for 1 h at 37°C. The monolayers were then washed three times with warm PBS and lysed with the addition of 450 μl/dish lysis buffer (0.4 M NaCl, 0.01 M Tris-HCl, pH 8.0, 5 mM EDTA, 0.2 mM PMSF, 5 mM *N*-ethylmaleimide, 1% NP-40, and 0.02% sodium azide).

To prepare immunoadsorbents, a series of tubes each containing 2-3 mg protein A-Sepharose 4B (Pharmacia Fine Chemicals) were each mixed with 25 μl rabbit anti-rat IgG (Fc fragment specific; Nordic Immunological Labs, Capistrano Beach, CA) in immunoprecipitation buffer (0.15 M NaCl, 0.01 M Tris-HCl, pH 8.0, 5 mM EDTA, 1% NP-40, 0.02% sodium azide).

After mixing for 90 min at room temperature, the beads were washed three times with immunoprecipitation buffer and then incubated overnight at 4°C with unlabeled parietal yolk sac (PYS)-2 cell lysate. Beads were then washed with immunoprecipitation buffer and then individual tubes were mixed with 25 μl of 3–6 mg/ml of one of the rat monoclonal or control IgGs for 90 min at room temperature. After three washes with immunoprecipitation buffer, tubes were then incubated for 90 min at room temperature with one of the radiolabeled PYS-2 cell lysates. Beads were washed three times with a mixture of 1.0 ml immunoprecipitation buffer and 450 μl of lysis buffer and finally with two washes of 0.01 M Tris-HCl, pH 6.8. Beads were then boiled in SDS sample buffer containing DTT. After cooling, samples were alkylated with 0.5 M iodoacetamide and electrophoresed in SDS gels with a 5–15% gradient of polyacrylamide (11). Coomassie brilliant blue-stained gels were soaked in Enlightning (Du Pont NEN Research Products) for 15 min before drying. Dried gels were then exposed to Kodak X-Omat (Eastman Kodak Co., Rochester, NY) film for 4–7 d at −70°C. Films were developed in Kodak D-19.

Immunoblotting Analysis

Nitrocellulose sheets onto which unreduced or reduced laminin had been electrotransferred from polyacrylamide gels were blocked with 5% solutions of nonfat powdered milk in PBS (BLOTTO [31]) and then sandwiched into a miniblotter apparatus (Immunetics, Cambridge, MA). Slots were treated sequentially with the rat monoclonal IgG fractions (100 μg/ml in BLOTTO) and affinity-purified goat anti-rat IgG coupled to horseradish peroxidase (HRP)[1] (Organon-Teknika-Cappel, Malvern, PA). Nitrocellulose sheets were then developed for peroxidase activity in 0.05% diaminobenzidine and 0.01% hydrogen peroxide (freshly diluted from a newly opened bottle of 30% H_2O_2) in 0.1 M phosphate buffer (23), pH 6.0. Electroblots of unreduced laminin P1 and unreduced elastase-digested laminin were also probed with rat mAbs.

Affinity Chromatography

Affinity columns were prepared by mixing 5 mg of anti-laminin mAb 5A2, 5C1, or 5D3 IgG with 3.0 ml of cyanogen bromide–activated Sepharose 4B (Pharmacia Fine Chemicals) in 0.1 M $NaHCO_3$, pH 8.3, containing 0.5 M NaCl for 2 h at room temperature. After washing with carbonate buffer, unreacted sites were blocked with 0.2 M glycine in carbonate buffer for 2 h. The coupled gels were then washed twice with carbonate buffer, once with 0.5 M NaCl in 0.1 M sodium acetate, pH 4.0, and finally resuspended in PBS containing 0.05% sodium azide and stored at 4°C. Approximately 3–4 mg elastase- or pepsin-digested laminin was passed over each column and bound fragments were eluted with 3 M potassium thiocyanate in 0.05 M phosphate buffer, pH 6.0. Eluted protein was dialyzed into either PBS, pH 7.3 or 0.2 M ammonium bicarbonate, pH 7.8.

Rotary Shadowing of Laminin and Monoclonal Anti-Laminin IgG Complexes

Mixtures containing undigested laminin, laminin P1, or elastase-generated laminin fragments (at concentrations of 0.1 μg/ml) and the mAbs (at concentrations of 50 μg/ml) were dialyzed against several changes of 0.2 M ammonium bicarbonate. Samples were mixed with equal volumes of glycerol and sprayed onto sheets of freshly cloven mica. The mica was then rotary shadowed with platinum at an angle of 9° and carbon at an angle of 90° in a vacuum coater (model E306A; Edwards High Vacuum, West Sussex, UK) operated at 1×10^{-5} Torr. Replicas were removed by floating onto distilled water, picked up on 400-mesh copper grids, and examined in a JEOL JEM-100 CX (JEOL USA, Peabody, MA) or Hitachi H-7000 (Hitachi Ltd., Tokyo) electron microscope.

Immunohistological Localization of the Anti-Laminin mAbs on Basement Membranes

Immunofluorescence Microscopy. A variety of unfixed tissue samples from mice were snap-frozen in isopentane chilled in a bath of dry ice and acetone and 4-μm-thick sections were cut at −20°C in a cryostat. Sections were air-dried at room temperature and then incubated sequentially with 50 μl/ml of one of the mAbs for 3–5 min followed by FITC-conjugated goat anti-rat IgG (Organon-Teknika-Cappel). Slides were examined by epifluorescence in a Leitz Orthoplan photomicroscope. In some cases, sections were treated for 5 min with 0.1 M acetic acid, 0.05 U/ml chrondroitinase ABC, or 1 m U/ml heparinase and 1 m U/ml heparitinase (ICN Biomedicals, Costa Mesa, CA) before immunolabeling. To screen the effects of fixation on binding of the mAbs, sections from mouse kidneys fixed with various dilutions of formaldehyde (freshly prepared from paraformaldehyde) and those fixed with paraformaldehyde-lysine-periodate (42) were also treated with mAbs and examined. In some experiments, 1.5–2.0 mg of the mAbs, in 0.02 M phosphate buffer, were intravenously injected via the saphenous vein into ether-anesthetized mice. At 1–3 h after injection, unfixed tissue samples were removed, frozen, and sectioned. In these cases, sections were incubated only with FITC-conjugated anti-rat IgG before examination.

Immunoperoxidase Electron Microscopy. Each mAb was coupled directly to activated HRP (Type VI, Sigma Chemical Co.) following the procedure of Nakane and Kawaoi (43). The conjugates were then screened for specificity on unfixed mouse kidney sections by immunofluorescence microscopy as described above. Each anti-laminin monoclonal mAb-HRP conjugate (at IgG concentrations of 2.0 mg/ml) was injected into at least two mice. 3 h after injection, kidneys were fixed by the subcapsular injection of 1.6% paraformaldehyde and 3% glutaraldehyde in 0.1 M sodium cacodylate buffer, pH 7.4 (Karnovsky's fixative). 40-μm-thick tissue slices were obtained with a Vibratome (Ted Pella, Inc., Redding, CA) and then processed for peroxidase histochemistry using the same conditions as for immunoblotting. Tissue was refixed for 2 h in 2% osmium tetraoxide, dehydrated, and embedded in epoxy. Ultrathin sections were stained for 30 s with lead citrate (51).

Results

Specificity of the Anti-Laminin IgGs

Of the 216 rat-mouse hybridomas screened, 19 were intensely positive by ELISA on laminin-coated wells and by immunofluorescence on mouse kidney basement membranes. Nine stable cell lines were eventually obtained through cloning that remained intensely positive by both of the above criteria. Isotyping showed that all of the clones were secreting rat IgG1, kappa. Specificity for laminin was initially demonstrated by inhibition ELISAs and binding of 0.5 μg/ml monoclonal rat IgG to laminin-coated microtiter plates was diminished 50% by preincubating the mAbs with soluble laminin at concentrations ranging from <1 μg/ml up to 25 μg/ml.

Specificity was further confirmed by immunoprecipitation of metabolically labeled laminin from PYS cell culture lysates. As shown in Fig. 1, all of the antibodies precipitated laminin specifically. Laminin A and B chains were recognized by all of the mAbs except 5A2, which precipitated only laminin B chains (Fig. 1). Binding was not eliminated in immunoprecipitation experiments from tunicamycin-treated PYS cultures (Fig. 1). Under these conditions, the A chain migrated faster and the B chains formed tighter bands in our gel system, indicating the efficacy of tunicamycin in at least reducing the amount of glycosylation. We were unable to clearly distinguish laminin B1 and B2 chains, however, on autoradiograms of tunicamycin-treated or untreated cultures. Control rat IgG did not precipitate any labeled PYS cell products.

Epitope Localization for the Anti-Laminin mAbs

All nine of the mAbs bound to unreduced tumor laminin on

1. *Abbreviations used in this paper*: GBM, glomerular basement membrane; HRP, horseradish peroxidase; mAb-LA, mAb binding to the end of the long arm of laminin; mAb-SA_1, and mAb SA_2, monoclonal antibodies binding to the short arms of laminin; parietal yolk sac; TBM, tubular basement membrane.

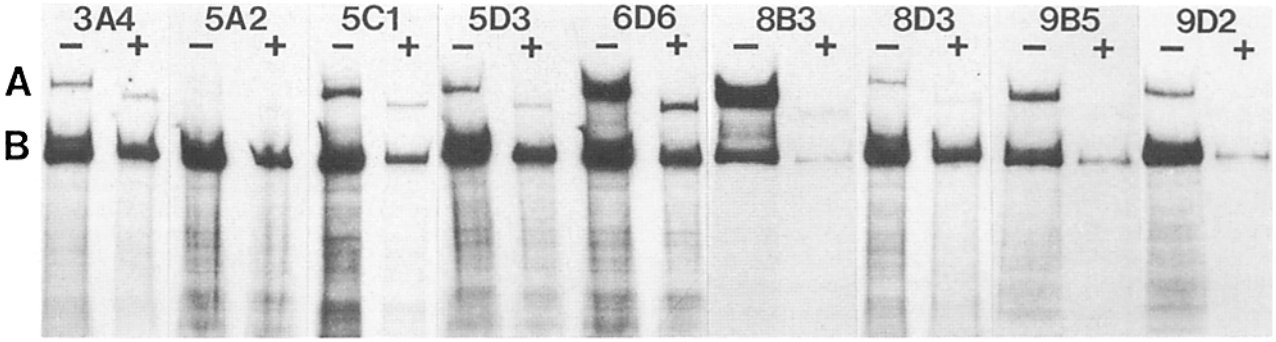

Figure 1. Autoradiogram of polyacrylamide gels showing the immunoprecipitation of [^{35}S]methionine-labeled laminin synthesized by cultured PYS cells. With the exception of mAb 5A2, all mAbs bind laminin A and B chains synthesized by cells in the absence of tunicamycin (−) and most also bind both chains in the presence of the drug (+).

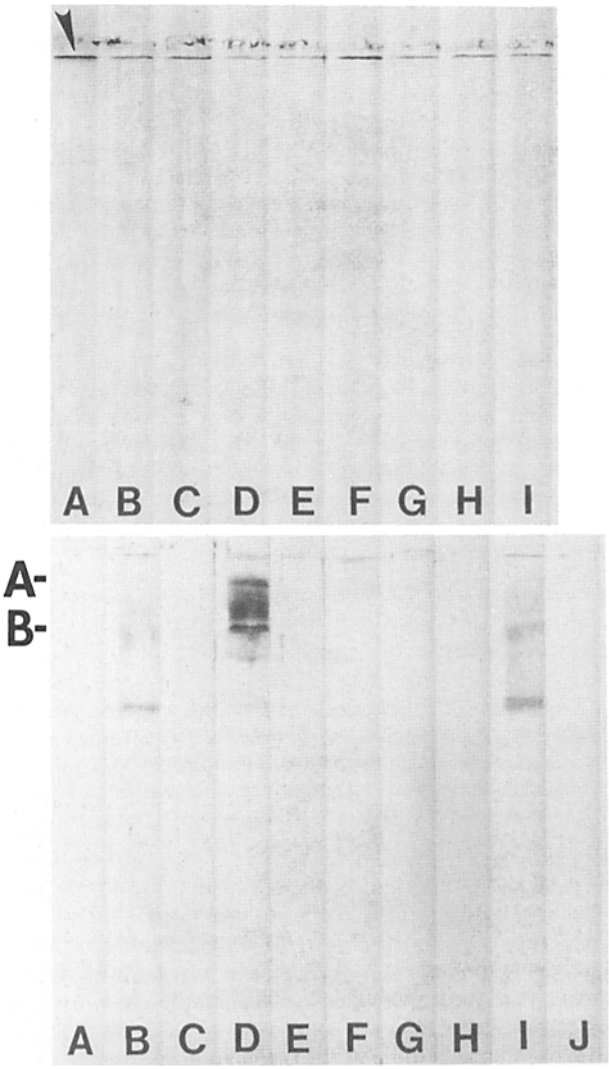

Figure 2. Immunoblots of laminin electrotransferred to nitrocellulose after SDS-PAGE under nonreducing (*top*) or reducing (*bottom*) conditions. (*Top*) All mAbs bind unreduced laminin (*arrowhead*). (*Bottom*) Three mAbs bind to reduced laminin. Locations of the laminin A and B chains are shown on the left. *A*, mAb 3A4; *B*, 5A2; *C*, 5C1; *D*, 5D3; *E*, 6D6; *F*, 8B3; *G*, 8D3; *H*, 9B5; *I*, 9D2; *J*, control rat IgG.

electroblots (Fig. 2) and three also bound to reduced laminin (Fig. 2). mAbs 5A2 and 9D2 bound to the B chains and what appeared to be proteolytic fragments thereof, whereas 5D3 bound to both A and B chains.

To localize the epitopes further, laminin was treated with pepsin and the P1 fragment was purified by gel filtration. mAbs 3A4, 5C1, 8B3, 8D3, and 9B5 bound to unreduced P1 on immunoblots (Fig. 3). Similarly, products from controlled elastase digestion of laminin (Fig. 4) were probed on immunoblots with the mAbs. Only mAb 5D3, which did not bind P1, bound to a ~140-kD (E8) fragment (Fig. 4, lane *4*). Although mAbs 5A2 and 9D2 did not bind to E8 or P1 on immunoblots, they did react with some other laminin fragments present in the crude elastase digest (Fig. 4, lanes *5* and *6*). When these fragments were isolated by mAb 5A2 affinity chromatography, however, mAb 5D3 did not cross-react with them (Fig. 4, lane *7*).

EM of rotary-shadowed immune complexes consisting of laminin and the mAbs allowed us to visualize directly some of the antibody binding sites. mAb 5A2 bound to a site on the inner globule of the short arms of intact laminin (Fig. 5). The distance from the center of the laminin cross to point of contact with mAb 5A2 measured 20.2 nm (±0.7 nm, n = 34). When the crude elastase digest was passed over an affinity column of mAb-5A2-Sepharose, large three-armed fragments containing globular domains were eluted with KSCN. As seen with intact laminin, mAb 5A2 also bound to an internal globule on the short arms of these fragments which measured 19.3 nm (±0.9 nm, n = 17) from the center of the cross (Fig. 5). mAb 5C1 bound to the lateral short arms near the center of the intact laminin cross (Fig. 6) and the same was true when 5C1 was mixed with purified P1 fragments (Fig. 6). These sites measured 18.1 nm (±1.0 nm, n = 19) from the center of the cross of intact laminin and 17.3 nm (±0.8 nm, n = 24) on P1 fragments. In contrast, mAb 5D3 bound 14.4 nm (±0.6 nm, n = 19) from the terminal globular domain on the long arm (Fig. 7). In addition, 5D3 also bound to a site 14.4 nm (±0.6 nm, n = 19) from the globular domain on purified E8 fragments of laminin eluted from a 5D3 affinity column (Fig. 7) and to the same sites on those eluted from heparin-Sepharose.

Antibody binding sites on the laminin molecule for the remaining six mAbs were not clearly resolved with the rotary shadowing technique. For some of these mAbs, our observa-

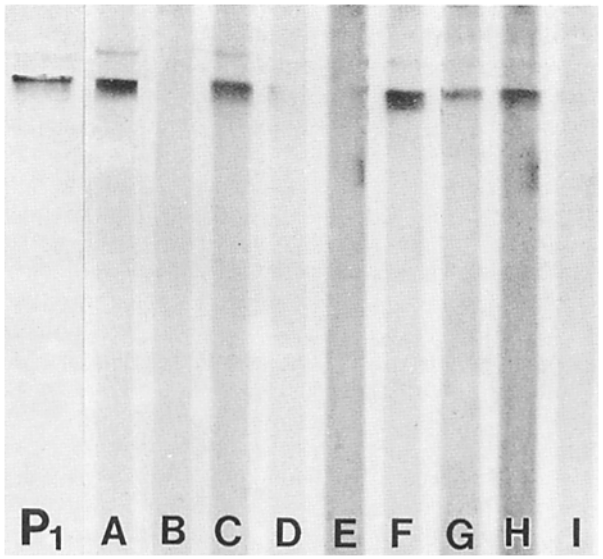

Figure 3. Immunoblot of laminin P_1 fragment after SDS-PAGE under nonreducing conditions. Coomassie brilliant blue–stained gel of P_1 is shown on the left. *A*, mAb 3A4; B, 5A2; *C*, 5C1; *D*, 5D3; *E*, 6D6; *F*, 8B3; *G*, 8D3; *H*, 9B5; *I*, 9D2.

tions suggested that the antibody binding sites on laminin were very near the center of the cross. However, this binding tended to obscure details, often resulting in a tangled appearance. On the other hand, mAbs 5A2, 5C1, and 5D3 bound at sites adequately distant from the center of the cross, thereby unequivocally locating their epitopes. A schematic diagram summarizing the binding sites for these mAbs is shown in Fig. 8. Hereafter, mAbs 5A2 and 5C1 will be referred to as mAbs-SA_1 and -SA_2, respectively, reflecting their localization to the short arms of laminin, and 5D3 will

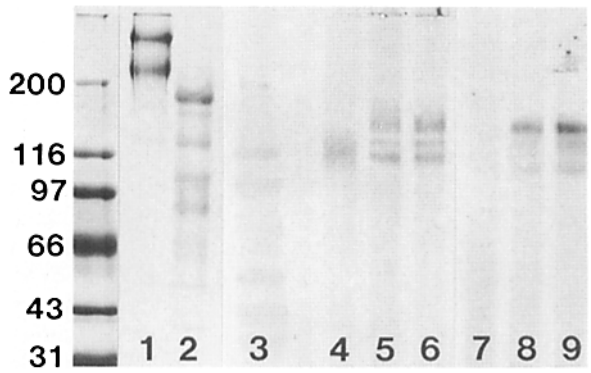

Figure 4. Lanes *1* and *2* show SDS-PAGE of reduced laminin and products after elastase digestion as described in Materials and Methods. Relative molecular weight $\times 10^3$ is shown on the left. (Lane *3*) Prestained relative molecular weight standards transferred to nitrocellulose. (Lane *4*) mAb 5D3 binds to a single band on an electroblot of the elastase digest. (Lanes *5* and *6*) mAbs 5A2 and 9D2 bind to several products in the elastase digest, but these differ from that recognized by mAb 5D3. (Lane *7*) mAb 5D3 does not bind to elastase fragments affinity isolated by mAb 5A2. (Lane *8* and *9*) mAbs 5A2 and 9D2 bind to elastase fragments affinity isolated by mAb 5A2.

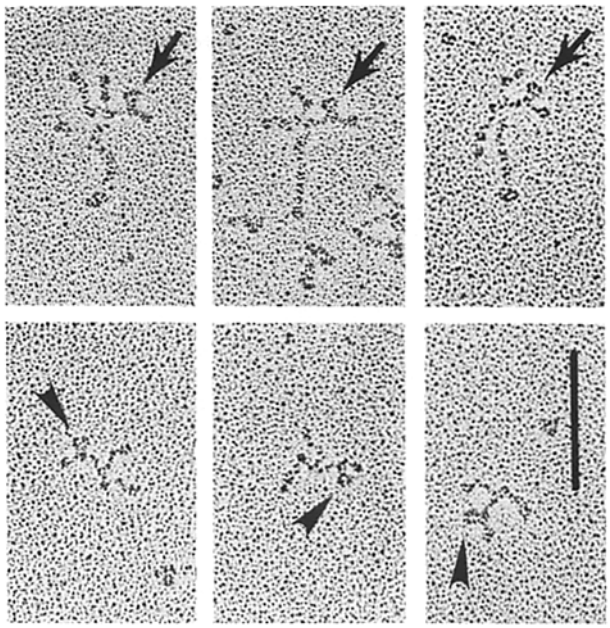

Figure 5. Electron micrographs of rotary-shadowed preparations consisting of mAb 5A2 and intact laminin (*top*) and elastase-generated fragments affinity isolated over a column of 5A2-Sepharose (*bottom*). mAb 5A2 binds to an internal globular domain on the short arms of intact laminin (*arrows*) and to corresponding sites on the elastase fragments (*arrowheads*). Scale bar, 100 nm.

be referred to as mAb-LA, reflecting its binding to the end of the long arm.

Immunofluorescence of Laminin with mAbs

All nine of the mAbs clearly reacted with mouse kidney tubular basement membranes (TBM) and glomerular mes-

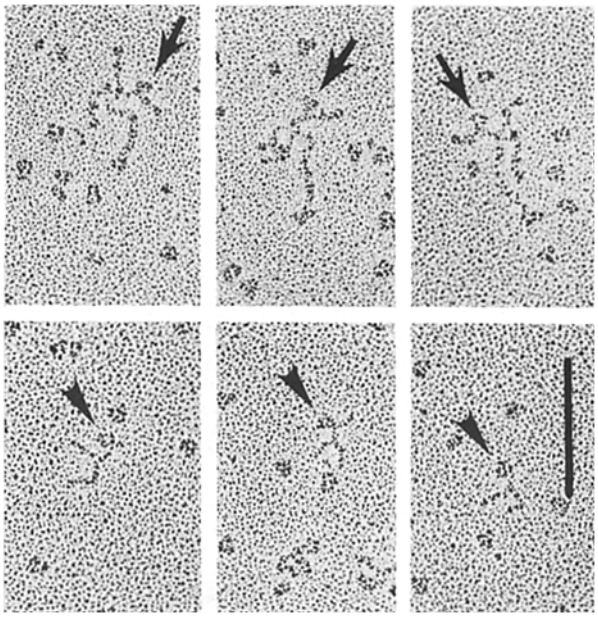

Figure 6. Micrographs of mAb 5C1 and intact laminin (*top*) and the P1 fragments obtained by gel filtration after pepsin digestion (*bottom*). MAb 5C1 binds to the short arms ~18 nm from the center of the laminin cross (*arrows*) and the same binding site is seen on P1 fragments (*arrowheads*). Scale bar, 100 nm.

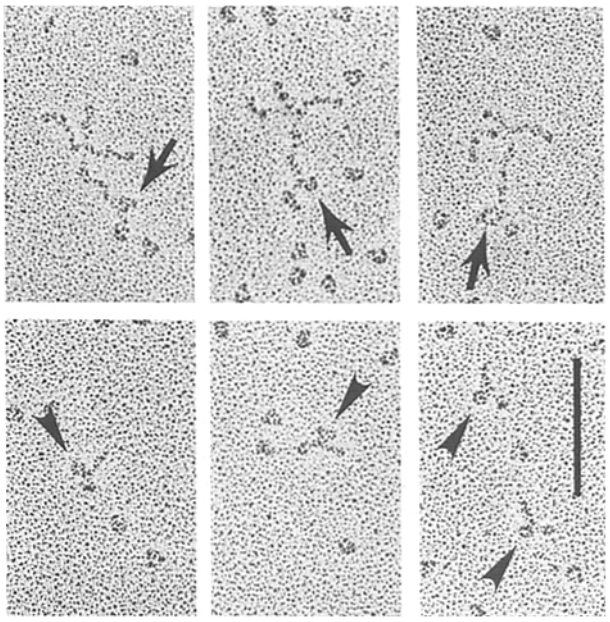

Figure 7. Micrographs of mAb 5D3 and intact laminin (*top*) and the E8 fragment obtained after elastase digestion and mAb 5D3 affinity chromatography (*bottom*). mAb 5D3 binds to an epitope located ~15 nm above the terminal globular domain of the long arm of laminin (*arrows*) and to the same site on E8 fragments (*arrowheads*). Scale bar, 100 nm.

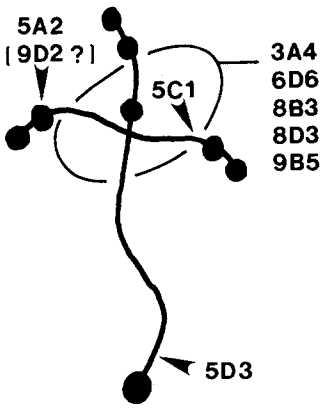

Figure 8. Schematic diagram of laminin showing the locations of binding sites for the mAbs. Epitopes for 5A2, 5C1, and 5D3 (*arrowheads*) were determined directly by rotary shadow EM with intact laminin and proteolytic digests. Because mAb 9D2 behaved exactly like 5A2 on immunoblots, we consider it likely that 9D2 maps near the same site. Locations for the remaining mAbs were inferred from blots of digests.

angial matrices as shown by immunofluorescence microscopy on sections of unfixed tissues, but there were some variations in labeling (Fig. 9). mAbs 8B3 and 8D3 bound only to some TBM, whereas the other mAbs appeared to label all TBM uniformly (Fig. 9). We obtained identical immunofluorescence results when cryostat kidney sections from mice that had received intravenous injections of mAbs were labeled directly with anti-rat IgG-fluorescein. In contrast, when cryostat sections from kidneys that had been fixed with 2% paraformaldehyde or the paraformaldehyde-lysine-periodate fixative were indirectly labeled, basement membrane fluorescence for all of the mAbs was either greatly diminished or abolished. Mild fixation with 1% paraformaldehyde did result in some basement membrane labeling, but the most intense fluorescence was always obtained on unfixed sections. The antibodies were also positive on unfixed cryostat sections of mouse peripheral nerve, smooth, skeletal, and cardiac muscle, and intestine, except for 8B3 and 8D3, which did not bind basement membranes in these sites (Fig. 10). In addition, attempts to "unmask" epitopes by pretreatment of cryostat sections with acetic acid, chondroitinase ABC, heparitinase, or heparinase failed to result in binding of 8B3 or 8D3 in these tissues.

Immunoelectron Microscopic Localization of Laminin

Two considerably different ultrastructural patterns of peroxidase reaction product were obtained in kidney basement membranes after the intravenous injection of different conjugates of monoclonal anti-laminin IgG-HRP. First, mAb-LA (5D3) bound in irregular patterns to the lamina rara interna of the peripheral loop glomerular basement membrane (GBM) (Fig. 11). The amount of reaction product within peripheral loop GBM was highly variable, ranging from spotty labeling as shown (Fig. 11) to no labeling. However, mesangial matrices, especially those areas immediately adjacent to mesangial cells, were consistently and densely labeled (Fig. 12). The lamina rara beneath the parietal epithelium of Bowman's capsule was specifically stained (Figs. 11 and 13) and dense labeling was also seen in the lamina rara along the proximal TBM (Figs. 14, *a* and *b*). Little or no staining of the lamina densa in the GBM, Bowman's capsule, or proximal TBM was obtained with mAb-LA (Figs. 11–14, *a* and *b*). By contrast, HRP reaction product was present through-

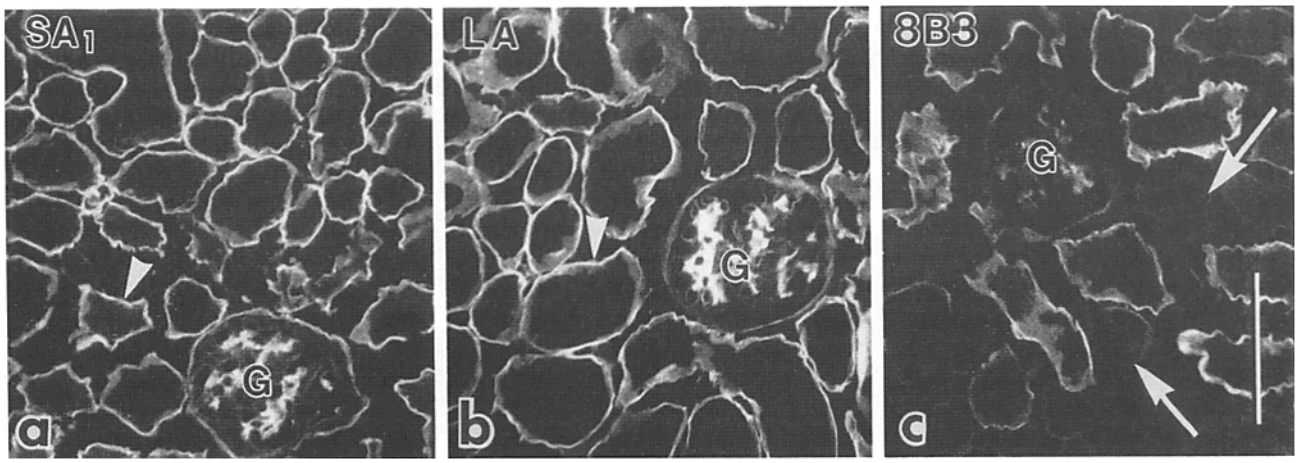

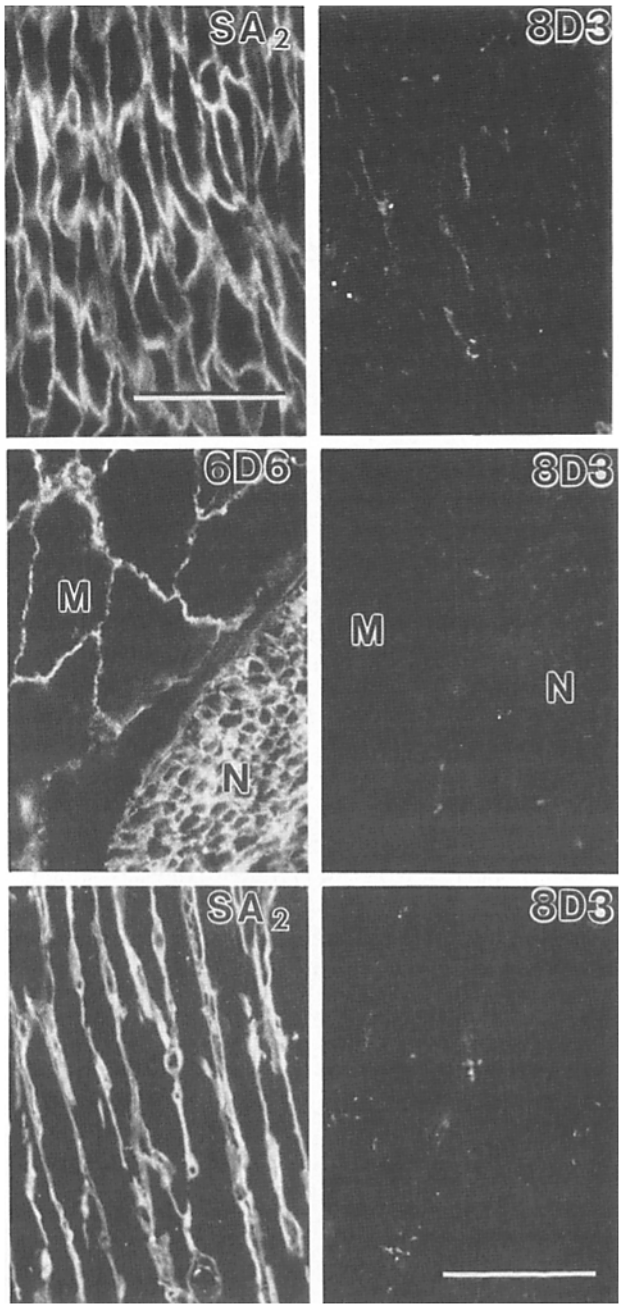

Figure 10. Immunofluorescence micrographs of cryostat sections taken of unfixed stomach smooth muscle (*top*), skeletal muscle (*M*) and peripheral nerve (*N*) (*middle*), and cardiac muscle (*bottom*) labeled with antibodies shown. Except for 8B3 and 8D3, all mAbs labeled mouse muscle and peripheral nerve basement membranes. Scale bar in *Top left*, 40 μm. All other figures were taken at the same magnification. Scale bar in *bottom right*, 100 μm.

out the lamina densa as well as the lamina rara in the basement membranes of the distal tubule (Figs. 11 and 14 *c*).

Results obtained with HRP conjugates prepared with mAbs 3A4, SA_1 (5A2), SA_2 (5C1), 6D6, 8D3, 9B5, and 9D2 were essentially similar. Within glomeruli, only occasional and nonlinear binding was seen in the peripheral loop GBM (Figs. 15 and 16), but all mAbs densely labeled the mesangial matrices (Fig. 15). As seen previously with mAb-LA, these mAbs also did not bind to the lamina densa of that part of the GBM that reflected over the mesangial matrix. In contrast to the dense staining seen with mAb-LA specifically in the lamina lucida of Bowman's capsule basement membrane (Figs. 11 and 13), these mAbs labeled Bowman's capsule in spotty patterns (Fig. 16). A similar spotty distribution was also seen in the TBM beneath the proximal tubule epithelium and discrete deposits of reaction product could often be detected in both the lamina rara and densa (Fig. 17 *a*). On the other hand, a dense, apparently even pattern of reaction product was seen throughout the lamina densa of the distal TBM (Fig. 17 *b*). Injections of 8B3-HRP resulted in apparently the same binding patterns as seen with these mAbs, but the peroxidase reaction product was much weaker in all locations. Perhaps the conjugation procedure affected the antigen-combining sites on mAb 8B3. Peroxidase reaction product was not present on the bases of foot processes or within the GBM, mesangial matrices, or other basement membranes in mice that received intravenous injections of control rat IgG-HRP (Fig. 18).

Discussion

Earlier immunofluorescence and immunoperoxidase studies have shown that various basement membranes are differentially immunoreactive to anti-laminin mAbs (25, 27, 29, 38, 63). In general, the previous immunoelectron microscopic reports have demonstrated that the relevant laminin epitopes are either present across the entire width of basement membranes or completely absent (29). Using peroxidase-conjugated mAbs mapped by rotary shadowing to different structural domains of laminin, however, our findings are the first to show that separate epitopes can be localized specifically to discrete sites within basement membranes.

On the basis of inhibition ELISAs, immunoprecipitation, electroblotting, and rotary shadowing of immune complexes, we conclude that the rat mAbs described here reacted specifically with mouse tumor laminin. Consistent with their sensitivities to aldehyde fixation, the epitopes recognized by these antibodies were probably proteinaceous, because laminin secreted by tunicamycin-treated PYS cells was immunoprecipitated. Most of the mAbs immunoprecipitated laminin A and B chains and mAb-LA also immunoblotted both chains. These results therefore indicate that similar if not identical epitopes were present on different laminin polypeptides. Owing to the close sequence homology between the B1, B2, and A chains (24, 49, 53–55), this is perhaps not surprising and others have likewise found that anti-laminin mAbs bind laminin A and B chains (27, 47, 59).

What do these experiments tell us about the molecular architecture of basement membranes? First, we interpret our immunoultrastructural detection of mAb-LA specifically

Figure 9. Immunofluorescence micrographs of cryostat sections taken from unfixed mouse kidneys labeled sequentially with rat anti-laminin mAbs and goat anti-rat IgG-fluorescein. *a* and *b* are labeled with mAbs SA_1 and LA, respectively, and show intense linear fluorescence of all TBM (*arrowheads*) and mesangial matrices of glomeruli (*G*). *C* shows labeling with mAb 8B3 where TBMs in some tubules are not labeled (*arrows*). Glomerular (*G*) labeling with mAb 8B3 is also relatively weaker than what is seen with mAbs SA_1 and LA. Scale bar, 100 μm.

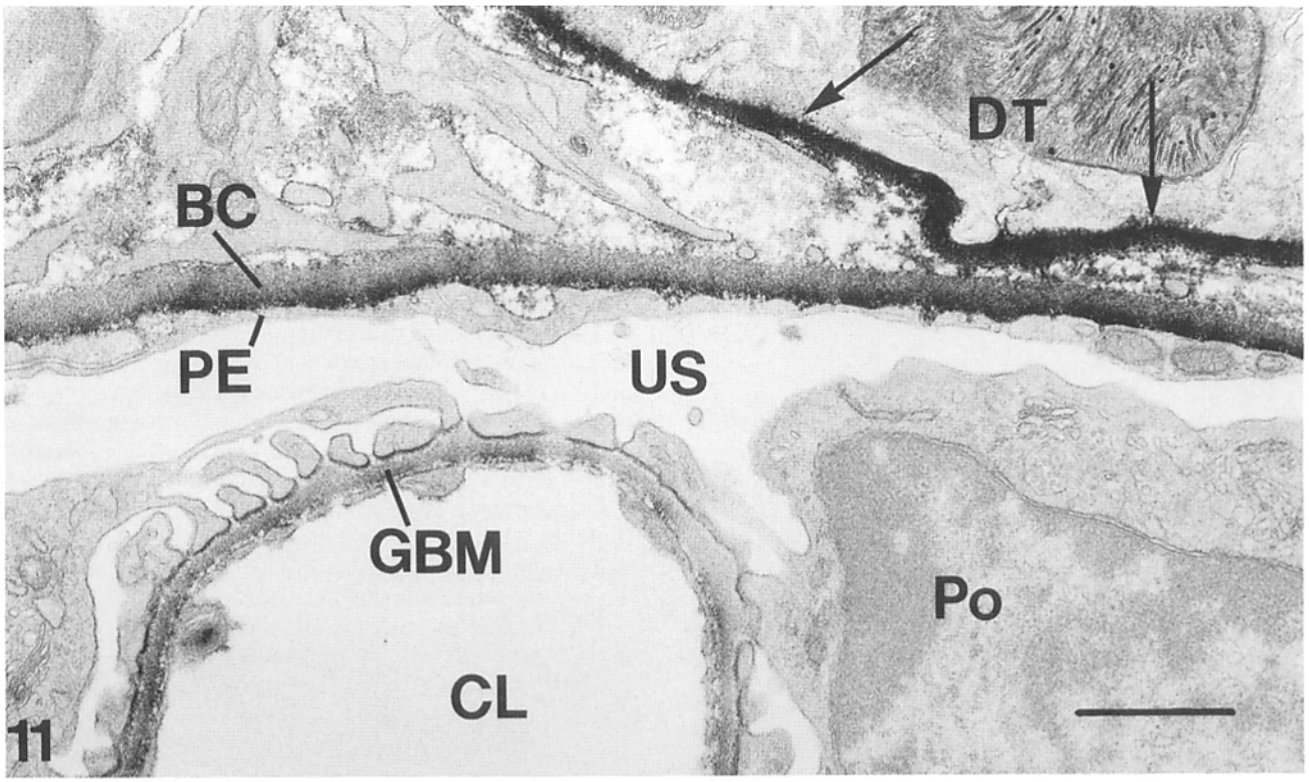

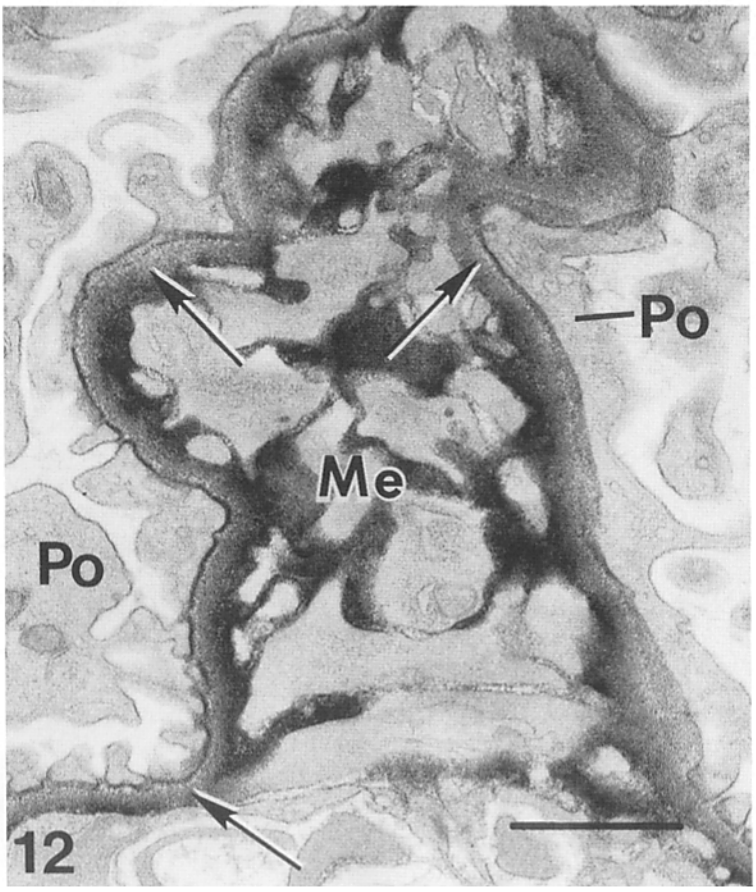

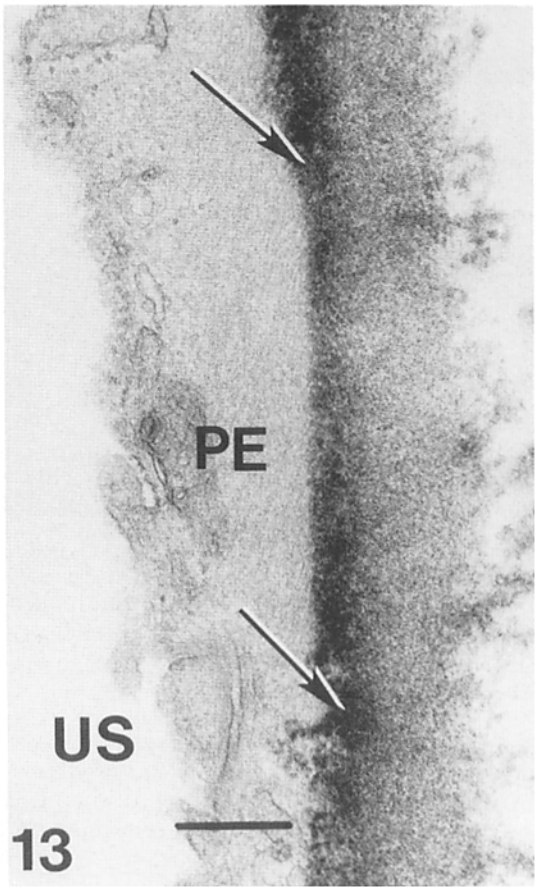

Figures 11–13. Electron micrograph of mouse kidney 3 h after intravenous injection with mAb-LA-HRP. Some peroxidase reaction product is seen within the lamina rara interna of the GBM. The innermost layer of Bowman's capsule basement membrane (*BC*) adjacent to the parietal epithelium (*PE*) is also specifically labeled, whereas TBM beneath the distal tubule epithelium (*DT*) is stained across its full width (*arrows*). *CL*, capillary lumen; *Po*, podocyte; *US*, urinary space. Scale bar, 1 μm. (*Figure 12*) Micrograph showing mesangial distribution of mAb-LA-HRP 3 h after injection. The matrix adjacent to mesangial cells (*Me*) is densely labeled. There is little or no binding of mAb-LA

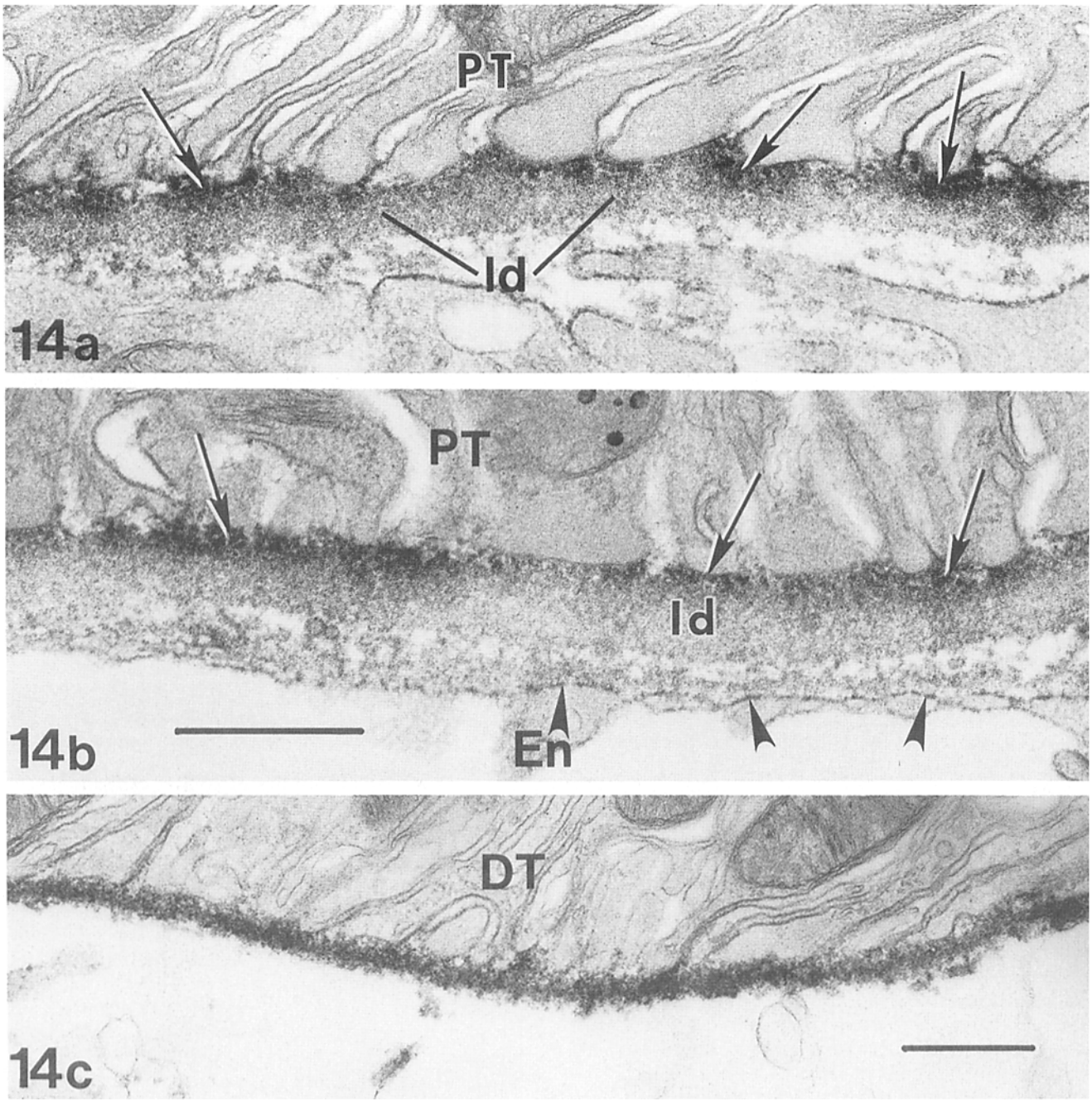

Figure 14. Micrographs showing the labeling of TBM in different regions of the nephron by injections of mAb-LA-HRP. In the proximal convoluted tubule (*a* and *b*), mAb-LA localizes only to the lamina rara (*arrows*) immediately beneath the basal labyrinth of proximal tubule epithelial cells (*PT*). The lamina densa of the TBM is unstained. Note that there appears to be a small amount of reactivity (*arrowheads*) in the lamina rara of the thin basement membrane beneath the endothelium (*En*) (*b*). Scale bar (*a* and *b*), 0.5 μm. In contrast, in the distal tubule (*c*), mAb-LA binds uniformly across the full thickness of the basement membrane beneath the distal tubule epithelium (*DT*). Scale bar, 0.5 μm.

within the lamina lucida of Bowman's capsule and the proximal TBM to indicate that the long arms of at least some laminin molecules are present directly beneath the basal plasma membranes of kidney epithelial cells. Due to the possibility that laminin assumes multiple orientations, the long arms of other laminin molecules may extend in an opposite direction into the lamina densa. Epitopes for mAb-LA were not detected in the lamina densa in these basement mem-

to the lamina densa (*arrows*) of the GBM reflecting over the mesangial matrix. *Po*, podocytes. Scale bar, 1 μm. (*Figure 13*) Higher power view of Bowman's capsule showing in vivo labeling with mAb-LA-HRP. Only the innermost layer of Bowman's capsule basement membrane is labeled (*arrows*). *US*, urinary space; *PE*, parietal epithelium. Scale bar, 0.25 μm.

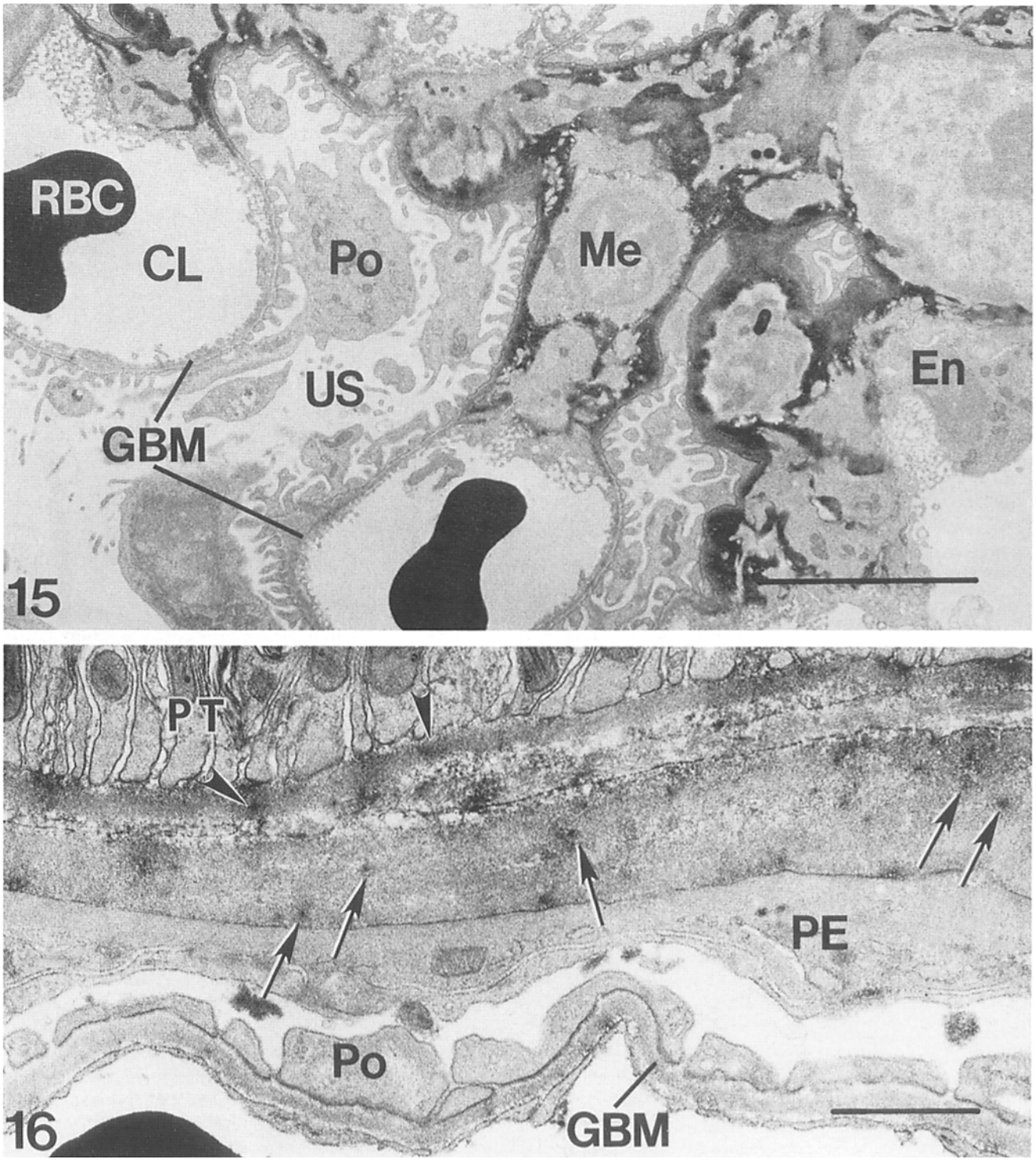

Figures 15 and 16. Glomerulus from a mouse that received mAb SA_1-HRP 3 h before fixation. Peroxidase reaction product is seen in matrices adjacent to mesangial cells (*Me*) but is generally absent in the peripheral loop GBM. *CL*, capillary lumen; *RBC*, erythrocyte; *En*, endothelium; *Po*, podocyte; *US*, urinary space. Scale bar, 5 μm. (*Figure 16*) Micrograph showing a general absence of binding of mAb SA_1-HRP to the peripheral loop GBM and a spotty distribution of peroxidase reaction product across the full width of Bowman's capsule basement membrane (*arrows*). Small spots of reactivity are also seen in the proximal TBM (*arrowheads*). *Po*, podocyte foot processes; *PE*, parietal epithelium; *PT*, proximal tubule epithelium. Scale bar, 1 μm.

branes, however, perhaps because of masking by other components. Our results nevertheless indicate striking immunoreactivity differences for laminin in different strata of certain basement membranes. Furthermore, they suggest that at least some normal epithelial cells may use the end of the long arm of laminin for basement membrane attachment in vivo. Additional support for this possibility comes from recent studies showing that chymotrypsin-generated laminin frag-

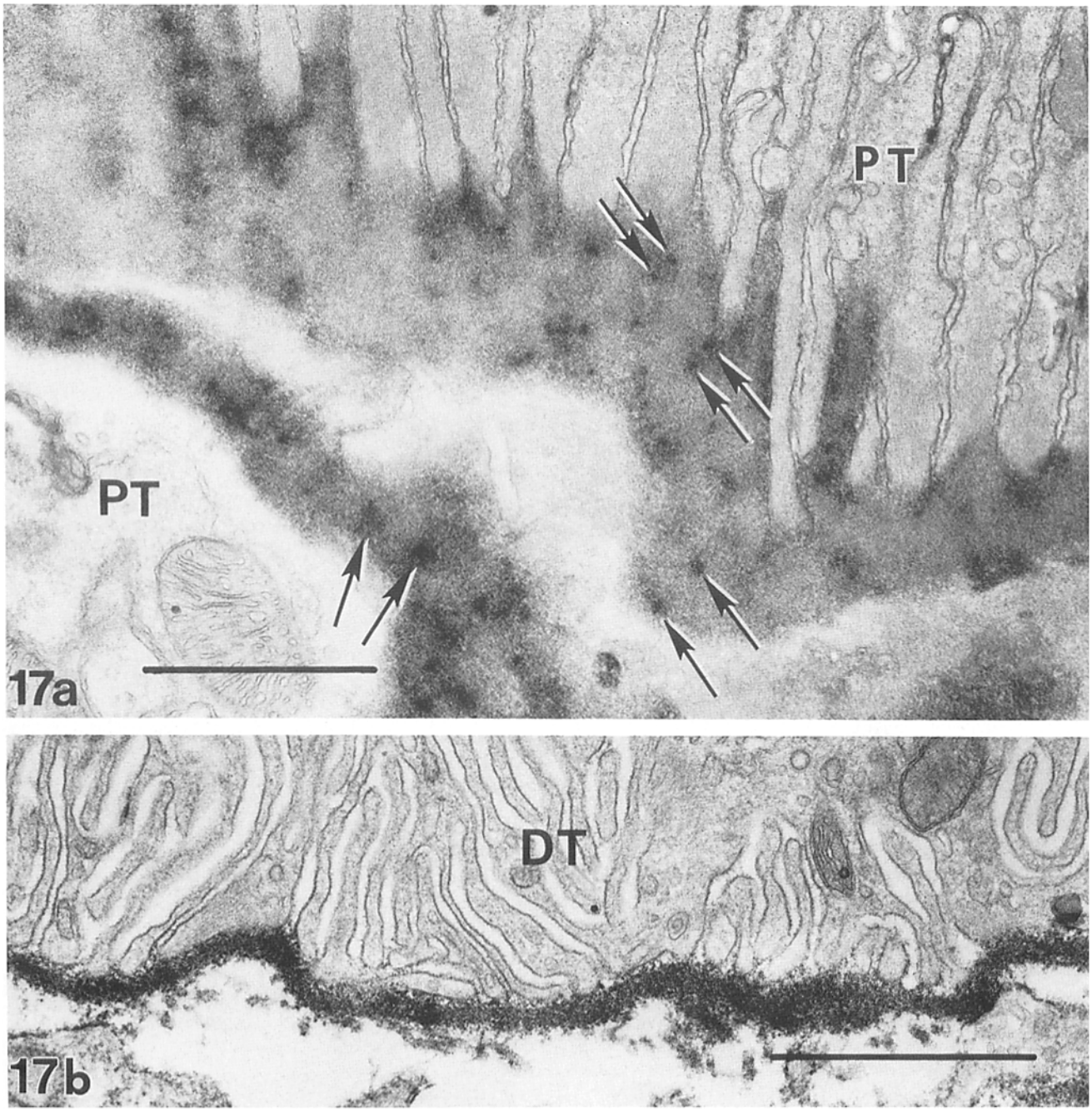

Figure 17. Representative micrographs showing the distribution of mAbs against laminin short arms in TBM of different regions of the nephron. (*a*) Tangential section across TBM of proximal tubule (*PT*). Binding of mAb 9D2-HRP to the TBM is seen as discrete, sometimes semiregular deposits of reaction product (*arrows*). Scale bar, 1 μm. (*b*) In contrast, all mAbs bound apparently evenly across the full width of distal tubule (*DT*) basement membranes and spotty reaction patterns were not observed. Shown here is distribution of mAb-SA_2-HRP. Scale bar, 1 μm.

ments, which contain the terminal globule of the long arm and promote neurite outgrowth in culture, also mediate the attachment and spreading of a number of different nonneuronal cell lines in vitro (13). Antisera directed specifically against the end of the long arm inhibits embryonic kidney epithelial cell polarization in vitro, further implicating a role for this domain of laminin in cell adhesion (34). In addition, recent studies have clearly demonstrated the specific binding of HT-1080 fibrosarcoma cells to native laminin via interactions with the long arm, E8 fragment (45). Because some previous investigations with polyclonal anti-laminin antibodies localized laminin mainly to the laminae rarae of the GBM (12, 18), perhaps the polyspecific IgGs used in these earlier experiments were directed primarily against the end of long arm. In contrast, in the basement membranes beneath the distal tubule epithelium, peroxidase reaction product from mAb-LA-HRP was found throughout the lamina rara and lamina densa, reflecting a localization of the end of the long arm to both sites in this basement membrane.

A clear interpretation of the results with antibodies that

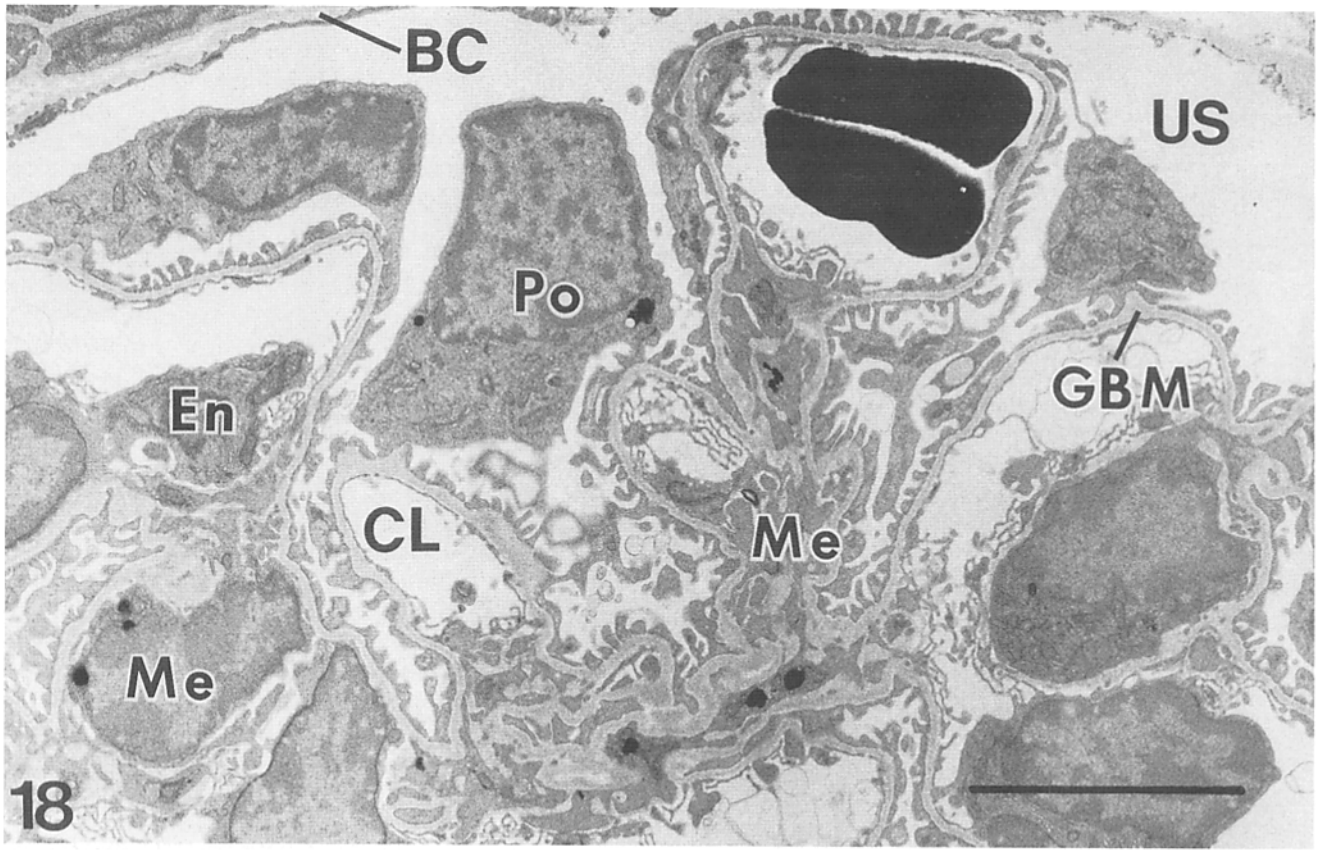

Figure 18. Glomerulus from a mouse that received an injection of control rat IgG-HRP 3 h before fixation. Reaction product is completely absent in GBM, mesangial matrices and Bowman's capsule (*BC*) basement membranes. *CL*, capillary lumen; *En*, endothelium; *Me*, mesangium; *Po*, podocyte. Scale bar, 5 μm.

mapped near the center of the laminin cross, including mAb-SA_1 and -SA_2, which bound on the short arms, is much more difficult to reach. All of these mAbs immunolocalized specifically and intensely across the lamina densa of distal tubule basement membranes. On the other hand, because the epitopes for these same antibodies were scattered in discrete spots across the basement membranes of the proximal tubule and Bowman's capsule, we conclude again that the molecular organization of basement membranes in these latter sites was therefore different. The distribution of distinct deposits of peroxidase across the multilayered Bowman's capsule basement membrane (41) is particularly interesting in view of the finding that mAb-LA bound only to the innermost layer immediately beneath the parietal epithelium. The absence of labeling in any particular site could have been due to masking of epitopes by other components or to a change in conformation of laminin. Nevertheless, whereas our results with mAb-LA demonstrated immunoreactivity differences in a vertical plane between the lamina rara and densa, our findings with these other mAbs are intriguing because they demonstrate that microdomains with different immunoreactivities exist laterally within basement membranes. In addition, these immunolocalization results are noteworthy since earlier studies have shown that the pepsin resistant, cross-shaped laminin P1 fragment mediates substrate adhesion for a number of different tumor cells and cell lines in vitro (40, 61). Further, various synthetic peptides corresponding to unique structural domains deduced from cDNA clones of the laminin B1 chain have been tested for cell binding activities. A sequence of five amino acids (YIGSR) that resides on the short arm of the B1 chain near the center of the cross, has been shown to promote tumor cell adhesion in vitro, and bind to a 67-kD laminin-binding protein isolated from tumor cell membranes (21, 22). Consequently, one might predict that the lamina rara would be particularly enriched with the P1 domain of laminin. We recognize that, if kidney epithelial cells were indeed adhering to laminin via interactions with the P1 domain, some of the epitopes for the mAbs would possibly be obscured. That none of the five different anti-P1 mAbs densely labeled the lamina rara, however, suggests that the P1 domain was not abundantly present in this layer. Moreover, some anti-laminin mAbs that block the adhesion of melanoma cells to laminin in vitro have been shown by rotary shadowing to bind to a region of the long arm extending beneath the center of the cross (59). In addition, an integrin-like receptor protein for laminin has been isolated from human glioblastoma cells that apparently does not interact with the YIGSR pentapeptide on the B1 chain of laminin (19), but may bind the RGD sequence in the A chain (55). This evidence, in conjunction with that discussed earilier on the ability of the end of the long arm of laminin to mediate cell adhesion, demonstrates that there are probably several distinct cell-binding regions on the laminin molecule and these seem to be distributed to different structural domains.

We do not consider an absence of mAb-HRP immunoreactivity within a particular layer of basement membrane to be

due to an artifact or lack of penetration of our immunoreagents for several reasons. First, we have previously shown that affinity purified, polyclonal anti-laminin IgG-HRP, in the same concentrations as used here for the monoclonal-HRP conjugates, binds throughout the full thickness of all vascular and epithelial basement membranes in organs fed by fenestrated or sinusoidal capillary systems (63). Here we observed that mAb-HRP conjugates yielded substantially different distribution patterns in different basement membranes. Second, our immunoperoxidase localization studies were conducted after the in vivo administration of antibodies, and binding therefore took place in the absence of fixatives of any kind. Indeed, for mAb-LA to bind almost exclusively to the lamina rarae of basement membranes beneath the parietal epithelium of Bowman's capsule or to renal proximal TBMs in vivo, the lamina densae of these same membranes must first have been crossed. Epitopes for mAb-LA, if present at all, were therefore not exposed in the lamina densa of these basement membranes. Similarly, epitopes for all of the monoclonal antibodies in the present analysis were undetectable in the lamina densa of peripheral loop GBM. This result is interesting because the GBM originates during nephrogenesis by the "fusion" of a double basement membrane beneath the vascular endothelium and visceral epithelium, respectively (reviewed in reference 4). Perhaps certain epitopes on laminin are masked or removed during this fusion process, and we are presently examining these possibilities.

Our mAb immunolocalization results partially agree with those obtained with polyclonal antibodies prepared against different structural domains of laminin. The latter studies have been conducted on mouse cornea and identify the center of the laminin cross primarily in the lamina densa and the end of the long arm mainly in the lamina rara (57). Unlike our findings in the kidney, however, the end of the long arm is also seen at the interface between the lamina densa and underlying stroma in the cornea (57). Earlier studies have also shown that different mouse anti-laminin mAbs bind selectively to different human basement membranes. One apparently binds all epithelial, muscle, and peripheral nerve basement membranes whereas another reacts with only some epithelial and vascular endothelial basement membranes (38). Some of these antibodies have also delineated a change in laminin immunoreactivities with development: early embryonic basement membranes are negative but become progressively positive with maturation (25). Similarly, two rat mAbs that bind different epitopes on mouse laminin B chains react in different patterns with basement membranes (29). One of these antibodies binds all kidney GBM and TBM, whereas another binds only the TBM beneath proximal convoluted tubules and the thin and thick ascending segments of Henle's loop (29). An analogous heterogeneity in mouse kidney basement membranes has been detected using immunofluorescence microscopy and anti-mouse tumor laminin mAbs (27). mAbs against a laminin homologue termed s-laminin also selectively stain certain basement membranes, particularly those in synaptic clefts and GBM (28). A quantitative immunocytochemical study with polyclonal antibodies against laminin and other basement membrane proteins also shows a heterogeneous distribution of these molecules in various kidney basement membranes (12a). The observed differences in immunoreactivities between various basement membranes indicates that some of the laminin epitopes are either absent in certain matrices, or masked by other components and therefore unavailable for binding. Our attempts to unmask cryptic epitopes with acid or enzymatic treatments were unsuccessful, however.

We believe that there are only two possible explanations for the observations discussed here. First, the molecular orientation or intercalation of laminin into basement membranes may vary with location. Further, these variabilities could also exist in separate layers or planes within the same basement membrane. Alternatively, there may be several genetically distinct isoforms of laminin distributed to different locales (28). In addition to the heterogeneity of laminin, selective binding to various basement membranes of mAbs against human collagen type IV (56) or uncharacterized human basement membrane components (25) have been observed previously. Differences have also been seen with polyclonal antibodies against the core protein of a rat basement membrane heparan sulfate proteoglycan (11). Together, all of the results strongly indicate that basement membranes in different locations are structurally unique. Whether these differences are related to the adhesive, permeability, or informational properties of basement membranes must now be established.

We are grateful to Dr. John Kearney for help with immunizations and advice on the rat-mouse fusion and to Fran Allen for technical assistance in culturing the hybridomas. We also thank Maxine Rudolph for secretarial help in preparing the manuscript.

These experiments were funded by grants DK-34972, DK-39258, and AR-36457 from the National Institutes of Health (NIH) and a grant-in-aid from the American Heart Association. The Hybridoma Core Facility of the Multi-purpose Arthritis Center at the University of Alabama at Birmingham is supported in part by grant 5P60 AR-20614-11 from the NIH. M. H. Irwin holds a Fellowship from the American Heart Association, Alabama Affiliate. D. R. Abrahamson is an Established Investigator of the American Heart Association.

Received 6 January 1989 and in revised form 10 September 1989.

References

1. Abrahamson, D. R. 1985. Origin of the glomerular basement membrane visualized after the in vivo labeling of laminin in newborn rat kidneys. *J. Cell Biol.* 100:1988–2000.
2. Abrahamson, D. R. 1986. Recent studies on the structure and pathology of basement membranes. *J. Pathol. (Lond.).* 149:257–278.
3. Abrahamson, D. R. 1986. Post-embedding colloidal gold immunolocalization of laminin to the lamina rara interna, lamina densa, and lamina rara externa of renal glomerular basement membranes. *J. Histochem. Cytochem.* 34:847–853.
4. Abrahamson, D. R. 1987. Structure and development of the glomerular capillary wall and basement membrane. *Am. J. Physiol.* 253 (*Renal Fluid Electrolyte Physiol.* 22):F783–F794.
5. Abrahamson, D. R., and J. P. Caulfield. 1982. Proteinuria and structural alterations in rat glomerular basement membranes induced by intravenously injected anti-laminin immunoglobulin G. *J. Exp. Med.* 156:128–145.
6. Abrahamson, D. R., and J. P. Caulfield. 1985. Distribution of laminin within rat and mouse renal, splenic, intestinal, and hepatic basement membranes identified after the intravenous injection of heterologous anti-laminin IgG. *Lab. Invest.* 52:169–181.
7. Barlow, D. P., N. M. Green, M. Kurkinen, and B. L. M. Hogan. 1984. Sequencing of laminin B chain cDNAs reveals C-terminal regions of coiled-coil alpha helix. *EMBO (Eur. Mol. Biol. Organ.) J.* 3:2355–2362.
8. Brazel, D., R. Pollner, I. Oberbaumer, and K. Kuhn. 1988. Human basement membrane collagen (type IV). The amino acid sequence of the alpha 2 (IV) chain and its comparison with the alpha 1 (IV) chain reveals deletions in the alpha 1 (IV) chain. *Eur. J. Biochem.* 172:35–42.
9. Charnois, A. S., E. C. Tsilibary, T. Saku, and H. Furthmayr. 1986. Inhibition of laminin self-assembly and interaction with type IV collagen by antibodies to the terminal domain of the long arm. *J. Cell Biol.* 103: 1689–1697.

10. Charonis, A. S., E. C. Tsilibary, P. D. Yurchenco, and H. Furthmayr. 1985. Binding of laminin to type IV collagen: a morphological study. *J. Cell Biol.* 100:1848–1853.
11. Couchman, J. R. 1987. Heterogeneous distribution of a basement membrane heparan sulfate proteoglycan in rat tissues. *J. Cell Biol.* 105:1901–1916.
12. Courtoy, P. J., R. Timpl, and M. G. Farquhar. 1982. Comparative distribution of laminin, type IV collagen, and fibronectin in the rat glomerulus. *J. Histochem. Cytochem.* 30:874–886.
12a. Desjardins, M., and M. Bendayan. 1989. Heterogeneous distribution of type IV collagen, entactin, heparan sulfate proteoglycan, and laminin among renal basement membranes as demonstrated by quantitative immunocytochemistry. *J. Histochem. Cytochem.* 37:885–897.
13. Dillner, L., K. Dickerson, M. Manthorpe, E. Ruoslahti, and E. Engvall. 1988. The neurite-promoting domain of human laminin promotes attachment and induces characteristic morphology in non-neuronal cells. *Exp. Cell Res.* 177:186–198.
14. Durkin, M. E., B. B. Bartos, S.-H. Liu, S. L. Phillips, and A. E. Chung. 1988. Primary structure of the mouse laminin B2 chain and comparison with laminin B1. *Biochemistry.* 27:5198–5204.
15. Edgar, D., R. Timpl, and H. Thoenen. 1984. The heparin-binding domain of laminin is responsible for its effects on neurite outgrowth and neuronal survival. *EMBO (Eur. Mol. Biol. Organ.) J.* 3:1463–1468.
16. Engel, J., E. Odermatt, A. Engel, J. A. Madri, H. Furthmayr, H. Rohde, and R. Timpl. 1981. Shapes, domain organizations, and flexibility of laminin and fibronectin, two multifunctional proteins of the extracellular matrix. *J. Mol. Biol.* 150:97–120.
17. Engvall, E., T. Krusius, U. Wewer, E. Ruoslahti, S. Varon, and M. Manthorpe. 1986. Mapping of domains in human laminin using monoclonal antibodies: localization of the neurite promoting site. *J. Cell Biol.* 103: 2457–2465.
18. Farquhar, M. G. 1981. The glomerular basement membrane: a selective macromolecular filter. *In* Cell Biology of Extracellular Matrix. E. D. Hay, editor. Plenum Publishing Corp., NY. 335–378.
19. Gehlson, K. R., L. Dillner, E. Engvall, and E. Ruoslahti. 1988. The human laminin receptor is a member of the integrin family of cell adhesion receptors. *Science (Wash. DC).* 241:1228–1229.
20. Goldberg, M., and F. Escaig-Haye. 1986. Is the lamina lucida of basement membrane a fixation artefact? *Eur. J. Cell Biol.* 42:365–368.
21. Graf, J., Y. Iwamoto, M. Sasaki, G. R. Martin, H. K. Kleinman, F. A. Robey, and Y. Yamada. 1987. Identification of an amino acid sequence in laminin mediating cell attachment, chemotaxis, and receptor binding. *Cell.* 48:989–996.
22. Graf, J., R. C. Ogle, F. A. Robey, M. Sasaki, G. R. Martin, Y. Yamada, and H. K. Kleinman. 1987. A pentapeptide from the laminin B1 chain mediates cell adhesion and binds the 67,000 laminin receptor. *Biochemistry.* 26:6896–6900.
23. Graham, R. C., and M. J. Karnovsky. 1966. The early stages of absorption of injected horseradish peroxidase in the proximal tubules of mouse kidney. Ultrastructural cytochemistry by a new technique. *J. Histochem. Cytochem.* 14:291–302.
24. Hartl, L., I. Oberbaumer, and R. Deutzmann. 1988. The N terminus of laminin A chain is homologous to the B chains. *Eur. J. Biochem.* 173:629–635.
25. Hessle, H., L. Y. Sakai, D. W. Hollister, R. E. Burgeson, and E. Engvall. 1984. Basement membrane diversity detected by monoclonal antibodies. *Differentiation.* 26:49–54.
26. Hogan, B. L. M., A. R. Cooper, and M. Kurkinen. 1980. Incorporation into Reichert's membrane of laminin-like extracellular proteins, synthesized by parietal endoderm cells of the mouse embryo. *Dev. Biol.* 80:289–300.
27. Horikoshi, S., H. Koide, and T. Shirai. 1988. Monoclonal antibodies against laminin A chain and B chain in the human and mouse kidneys. *Lab. Invest.* 58:532–538.
28. Hunter, D. D., V. Shah, J. P. Merlic, and J. R. Sanes. 1989. A laminin-like adhesive protein concentrated in the synaptic cleft of the neuromuscular junction. *Nature (Lond.).* 338:229–234.
29. Jaffe, R., B. Bender, M. Santamaria, and A. E. Chung. 1984. Segmental staining of the murine nephron by monoclonal antibodies directed against the GP-2 subunit of laminin. *Lab. Invest.* 51:88–96.
30. Jaye, M., W. S. Modi, G. A. Ricca, R. Mudd, I. M. Chiu, S. J. O'Brien, and W. N. Drohan. 1987. Isolation of a cDNA clone for the laminin-B1 chain and its gene localization. *Am. J. Hum. Genet.* 41:609–615.
31. Johnson, D. A., J. W. Gautsch, J. R. Sportsman, and J. H. Elder. 1984. Improved technique utilizing nonfat dry milk for analysis of proteins and nucleic acids transferred to nitrocellulose. *Gene Anal. Tech.* 1:3–8.
32. Deleted in proof.
33. Kearney, J. F. 1984. Hybridomas and monoclonal antibodies. *In* Fundamental Immunology. W. E. Paul, editor. Raven Press, NY. 751–766.
34. Klein, G., M. Langegger, R. Timpl, and P. Ekblom. 1988. Role of laminin A chain in the development of epithelial cell polarity. *Cell.* 55:331–341.
35. Laurie, G. W., J. T. Bing, H. K. Kleinamn, J. R. Hassell, M. Aumailley, G. R. Martin, and R. J. Feldman. 1986. Localization sites for laminin, heparan sulfate proteoglycan and fibronectin on basement membrane (type IV) collagen. *J. Mol. Biol.* 189:205–216.
36. Laurie, G. W., C. P. Leblond, S. Inoue, G. R. Martin, and A. Chung. 1984. Fine structure of the glomerular basement membrane and immunolocalization of five basement membrane components to the lamina densa (basal lamina) and its extensions in both glomeruli and tubules of the rat kidney. *Am. J. Anat.* 169:463–481.
37. Lehman, J. M., W. C. Speers, D. E. Swartzendrubes, and G. B. Pierce. 1974. Neoplastic differentiation: characterizatics of cell lines derived from a murine teratocarcinoma. *J. Cell Physiol.* 84:13–28.
38. Leu, F. J., E. Engvall, and I. Damjanov. 1986. Heterogeneity of basement membranes of genitourinary tract revealed by sequential immunofluorescence staining with monoclonal antibodies to laminin. *J. Histochem. Cytochem.* 34:483–489.
39. Lieberman, R., and W. Humphrey. 1972. Association of H-2 types with genetic control of immune responsiveness to IgG (α2a) allotypes in the mouse. *J. Exp. Med.* 136:1222–1230.
40. Martin, G. R., and R. Timpl. 1987. Laminin and other basement membrane components. *Annu. Rev. Cell Biol.* 3:57–85.
41. Mbassa, G., M. Elger, and W. Kritz. 1988. The ultrastructural organization of the basement membrane of Bowman's capsule in the rat renal corpuscle. *Cell Tissue Res.* 253:151–163.
42. McLean, I. W., and P. K. Nakane. 1974. Periodate-lysine-paraformaldehyde fixative. A new fixative for immunoelectron microscopy. *J. Histochem. Cytochem.* 22:1077–1083.
43. Nakane, P. K., and A. Kawaoi. 1974. Peroxidase-labeled antibody. A new method of conjugation. *J. Histochem. Cytochem.* 22:1084–1091.
44. Nath, P., M. Laurent, E. Horn, M. E. Sobel, G. Zon, and G. Vogeli. 1986. Isolation of an alpha 1 type-IV collagen cDNA clone using a synthetic oligodeoxynucleotide. *Gene (Amst.).* 43:301–304.
45. Nurcombe, V., M. Aumailley, R. Timpl, and D. Edgar. 1989. The high-affinity binding of laminin to cells. Assignation of a major cell-binding site to the long arm of laminin and of a latent cell-binding site to its short arms. *Eur. J. Biochem.* 180:9–14.
46. Ott, U., E. Odermatt, J. Engel, H. Furthmayr, and R. Timpl. 1982. Protease resistance and conformation of laminin. *Eur. J. Biochem.* 123: 63–72.
47. Palm, S. L., J. B. McCarthy, and L. T. Furcht. 1985. Alternative model for the internal structure of laminin. *Biochemistry.* 24:7753–7760.
48. Paulsson, M., R. Deutzmann, R. Timpl, D. Dalzoppo, E. Odermatt, and J. Engel. 1985. Evidence for coiled-coil a-helical regions in the long arm of laminin. *EMBO (Eur. Mol. Biol. Organ.) J.* 4:309–316.
49. Pikkarainen, T., R. Eddy, Y. Fukishima, M. Byers, T. Shows, T. Pihlajaniemi, M. Saraste, and K. Tryggvason. 1987. Human laminin B1 chain. A multidomain protein with gene (LAMB1) locus on the q22 region of chromosome 7. *J. Biol. Chem.* 262:10454–10462.
50. Pikkarainen, T., T. Kallunki and K. Tryggvason. 1988. Human laminin B2 chain. Comparison of the complete amino acid sequence with the B1 chain reveals variability in sequence homology between different structural domains. *J. Biol. Chem.* 263:6751–6758.
51. Reynolds, E. S. 1963. The use of lead citrate at high pH as an electron opaque stain in electron microscopy. *J. Cell Biol.* 17:208–212.
52. Rohde, H., H. P. Bachinger, and R. Timpl. 1980. Characterization of pepsin fragments of laminin in a tumor basement membrane. Evidence for the existence of related proteins. *Hoppe-Seyler's Z. Physiol. Chem.* 361: 1651–1660.
53. Sasaki, M., S. Kato, K. Kohono, G. R. Martin, and Y. Yamada. 1987. Sequence of the cDNA encoding the laminin B1 chain reveals a multidomain protein containing cysteine-rich repeats. *Proc. Natl. Acad. Sci. USA.* 84:935–939.
54. Sasaki, M., H. K. Kleinman, H. Huber, R. Deutzmann, and Y. Yamada. 1988. Laminin, a multidomain protein. *J. Biol. Chem.* 263:16536–16544.
55. Sasaki, M., and Y. Yamada. 1987. The laminin B2 chain has a multidomain structure homologous to the B1 chain. *J. Biol. Chem.* 262:17111–17117.
56. Scheinman, J. I., and C. Tsai. 1984. Monoclonal antibody to type IV collagen with selective basement membrane localization. *Lab. Invest.* 50: 101–112.
57. Schittny, J. C., R. Timpl, and J. Engel. 1988. High resolution immunoelectron microscopic localization of functional domains of laminin, nidogen, and heparan sulfate proteoglycan in epithelial basement membrane of mouse cornea reveals different topological orientations. *J. Cell Biol.* 107:1599–1610.
58. Schwarz, U., D. Schuppan, I. Oberbaumer, R. W. Glanville, R. Deutzmann, R. Timpl, and K. Kuhn. 1986. Structure of mouse type IV collagen. Amino-acid sequence of the C-terminal 511-residue-long triple-helical segment of the alpha 2(IV) chain and its comparison with the alpha 1(IV) chain. *Eur. J. Biochem.* 157:49–56.
59. Skubitz, A. P. N., A. Charonis, E. C. Tsilibary, and L. T. Furcht. 1987. Localization of a tumor cell adhesion domain of laminin by a monoclonal antibody. *Exp. Cell Res.* 173:349–369.
60. Timpl, R., and M. Dziadek. 1986. Structure, development, and pathology of basement membranes. *Int. Rev. Exp. Pathol.* 29:1–112.
61. Timpl, R., S. Johansson, V. van Delden, I. Oberbaumer, and M. Hook. 1983. Characterization of protease resistant fragments of laminin mediating attachment and spreading of rat hepatocytes. *J. Biol. Chem.* 258: 8922–8927.

62. Timpl, R., H. Rohde, P. Gehron Robey, S. I. Rennard, J. M. Foidart, and G. R. Martin. 1979. Laminin: a glycoprotein from basement membranes. *J. Biol. Chem.* 254:9933–9937.
63. Wan, Y.-J., T.-C. Wu, A. E. Chung, and I. Damjanov. 1984. Monoclonal antibodies to laminin reveal the heterogeneity of basement membranes in the developing and adult mouse tissues. *J. Cell Biol.* 98:971–979.
64. Yurchenco, P. D., E. C. Tsilibary, A. S. Charonis, and H. Furthmayr. 1985. Laminin polymerization in vitro: evidence for a two-step assembly with domain specificity. *J. Biol. Chem.* 260:7636–7644.
65. Yurchenco, P. D., E. C. Tsilibary, A. S. Charonis, and H. Furthmayr. 1986. Models for the self-assembly of basement membrane. *J. Histochem. Cytochem.* 34:93–102.